Available online at www.sciencedirect.com

ScienceDirect

Geochimica et Cosmochimica Acta 280 (2020) 148–160

Geochimica et Cosmochimica Acta

www.elsevier.com/locate/gca

Temperature-induced iron (III) reduction results in decreased dissolved organic carbon export in subalpine wetland soils, Colorado, USA

Céline Pallud [a,*], Charles C. Rhoades [b], Linden Schneider [a], Pranjal Dwivedi [a], Thomas Borch [c]

[a] Department of Environmental Science, Policy and Management, University of California, Berkeley, 130 Mulford Hall, Berkeley, CA 94720, USA

[b] USDA Forest Service Rocky Mountain Research Station, 240 West Prospect Road, Fort Collins, CO 80526, USA

[c] Department of Soil and Crop Sciences and the Department of Chemistry, Colorado State University, Fort Collins, CO, 80523, USA

Received 13 September 2019; accepted in revised form 16 March 2020; Available online 5 April 2020

Abstract

Concentrations of dissolved organic carbon (DOC) in surface waters have rapidly increased across Europe and North America over the past few decades. The causes for such trends have yet to be fully understood, although several factors including elevated temperatures and decreased atmospheric deposition of acid, nitrogen and sulfur, are considered responsible for the release of carbon from soils into streams. In order to determine how seasonal temperature patterns and soil physical and chemical characteristics influence iron (Fe)(III) reduction and DOC release to pore-water in subalpine wetland soils, we measured potential Fe(II) and DOC export rates at low (6 °C) and high (18 °C) temperatures using flow-through reactors containing undisturbed wetland soils sampled in the Fraser Experimental Forest (Colorado, USA) in two wetland types and at two depths.

Higher temperature, soil organic matter, nitrogen, and extractable Fe concentrations, but lower soil C:N ratios and extractable manganese concentrations promoted Fe(II) export from soil to water. Additionally, Fe(III) reduction was 1.5–5 times more responsive to temperature in shallow, organic matter-rich soils, compared to organic-poor deeper soils. Conversely, DOC export declined at higher temperature in all soils, consistent with a temperature-related increase in carbon respiration by Fe(III)-reducers. While higher temperature is expected to reduce carbon storage in wetland soils, our findings suggest that temperature-related increase in Fe(III) reduction will not generate additional release of DOC from soils to rivers.

Keywords: Soil temperature; Water quality; Soil carbon storage; Reductive Fe(III) dissolution; Headwater dissolved organic matter

1. INTRODUCTION

Dissolved organic carbon (DOC) concentrations have increased significantly in many North American and European surface waters over the last two decades (Freeman et al., 2001; Freeman et al., 2004; Worrall et al., 2004; Evans et al., 2005; Findlay, 2005; Evans et al., 2006; Roulet and Moore, 2006; Clark et al., 2010; Knorr, 2013), leading to a range of potential environmental consequences, including effects on clarity and acidity, metal and contaminant mobility, as well as drinking water quality (Roulet and Moore, 2006; Knorr, 2013). Increased DOC export from snowmelt-dominated watersheds is of particular concern as these areas supply drinking water to over 1 billion people

* Corresponding author.
E-mail address: cpallud@berkeley.edu (C. Pallud).

https://doi.org/10.1016/j.gca.2020.03.023
0016-7037/

globally (Barnett et al., 2005). Transport of soil carbon (C) to surface water could also represent a critical reduction in terrestrial C reserves (Worrall et al., 2004; Scharlemann et al., 2014) or indicate an increased rate of C cycling in those stores (Worrall et al., 2004). The mechanisms leading to the observed rises in surface water DOC levels have been extensively debated (Evans et al., 2002; Tranvik and Jansson, 2002; Freeman et al., 2004; Worrall et al., 2004; Evans et al., 2005; Evans et al., 2006; Clark et al., 2010), and several interacting factors are probably involved. In catchment-scale studies, elevated temperature and CO_2 levels, altered hydrological patterns, declining atmospheric deposition of acid, nitrogen (N) and sulfur, which would increase the prevalence of iron (Fe) reduction, and altered soil redox status have all been suggested (Freeman et al., 2001; Freeman et al., 2004; Worrall and Burt, 2004; Roulet and Moore, 2006; Clark et al., 2010; Winterdahl et al., 2011; Knorr, 2013). In addition, a recent study showed that DOC flux was transport-limited in 80% of 1000 watersheds in the conterminous USA, and that the watershed slope was the most important predictor of DOC concentrations (Zarnetske et al., 2018).

Wetland soils contain 20–30% of the terrestrial C inventory despite their limited spatial extent (6–8% of Earth's land surface) (Carnell et al., 2018). Hydroperiod, hydraulic residence time, and hydrologic connectivity vary among distinct hydrogeomorphic wetland types (Brinson, 1993; Covino, 2017) and influence C storage and element cycling (Knorr et al., 2009; Segnini et al., 2010; Bernal and Mitsch, 2012; Ameli and Creed, 2017; Covino, 2017). For example, slow flow and persistent saturation create stable, anoxic conditions that favor organic matter (OM) accumulation (Maltby and Barker, 2009). Soil mineralogy, microbial community composition, and OM content regulate the supply of terminal electron acceptors and C for anaerobic respiration (Grybos et al., 2007; Grybos et al., 2009; Knorr et al., 2009; Maltby and Barker, 2009; Clark et al., 2010; Mills et al., 2014). Iron (Fe) oxide minerals stabilize substantial amounts of C in natural soils and sediments due to their high sorption capacity and because of co-precipitation between OM and Fe-oxides (Kaiser and Guggenberger, 2007; Wagai and Mayer, 2007; Lalonde et al., 2012; Mu et al., 2016). As a result, up to 20% of the organic C in marine sediments is associated with Fe minerals (Lalonde et al., 2012). Under acidic conditions in wetland soils, ligand exchange between OM functional groups and Fe-oxide surfaces is the dominant sorption mechanism (Gu et al., 1994) relative to others processes such as anion exchange, hydrophobic interactions, hydrogen bonding, cation bridging, and entropic effects. Microbially-mediated Fe(III) reduction is responsible for C oxidation under anoxic conditions, and abiotic and biotic dissolution of Fe(III) minerals can release mineral-associated C (Kritzberg and Ekström, 2012; Knorr, 2013; Herndon et al., 2015; Pan et al., 2016; Herndon et al., 2017). However, dissimilatory Fe(III) reduction may not always lead to release and loss of C, especially when Fe minerals are co-precipitated with C (Shimizu et al., 2013). Indeed, co-precipitated OM may influence the rates, pathway and products of microbial Fe(III) reduction in soils (Peiffer et al., 1999; Amstaetter et al., 2012; Shimizu et al., 2013). Suppression of Fe(III) reduction by co-precipitated humic acids or fulvic acids has been observed under simplified laboratory conditions (Eusterhues et al., 2014; Mejia et al., 2018; Zhou et al., 2018). Owing to the large inventory of C stored in wetlands it is critical that we fully understand the link between reductive Fe(III) mineral dissolution and DOC release in wetland soils.

Simultaneous increases in Fe(II) and DOC concentrations have been documented in surface waters throughout Europe (Olivie-Lauquet et al., 2001; Kritzberg and Ekström, 2012; Knorr, 2013; Emsens et al., 2016; Björnerås et al., 2017), yet the explicit role of temperature on this pattern remains uncertain. However, increased DOC loadings to surface waters have been suggested to originate from intense mobilization of DOC in adjacent wetland and riparian soils (Hemond, 1990; Schiff et al., 1997; Hinton et al., 1998; Morel et al., 2009; Knorr, 2013; Riedel et al., 2013). In this study, we evaluated the influence of temperature and soil physical and chemical characteristics, including pH, OM and macro- and micro-nutrient contents, on Fe(II) and DOC export from soil to pore-water. Specifically, we measured rates of Fe(II) and DOC export using flow-through reactors (FTR) containing intact soil slices sampled in two wetlands with distinct hydrogeomorphic conditions and hydroperiods. FTRs containing undisturbed soil samples preserve the pore structure and the spatial distribution of solid-bound constituents, including microorganisms and substrates, thereby providing a simple means of determining reaction rates under conditions that more closely reflect the initial *in situ* conditions than would well-mixed batch experiments (Pallud and Van Cappellen, 2006). This study will improve understanding of the mechanisms that regulate soil C and Fe release from wetland soils to surface- or pore-water under seasonal temperature variations.

2. MATERIALS AND METHODS

2.1. Study sites and soil sampling

We compared soils from two contrasting subalpine wetlands; a slope wetland and a depressional wetland (Fig. 1), at the United States Department of Agriculture (USDA) Forest Service, Fraser Experimental Forest (FEF), 137 km west of Denver, Colorado, USA (Nelson et al., 2011; Daugherty et al., 2019). Soil temperatures in a similar subalpine forest located 10 km from our field sites reached 19 °C in summer and ranged between 5 and 10 °C in spring and fall (Rhoades et al., 2012).

The slope wetland is located at 39°53′6.90″N, 105°51′43.90″W (3020 m) on a hillslope of 15–20%. This groundwater-fed wetland has a short hydrologic residence time (hours to days), and a permanent inundation. Due to the uniformity in inundation (Daugherty et al., 2019), we sampled a single site in the center of the wetland (Fig. 1A and B). The depressional wetland is located at 39°54′31.91″N, 105°51′51.45″W (2800 m). This snowmelt-fed wetland is characterized by a longer hydrologic residence time (months) and heterogeneity in inundation. We sampled two sites along

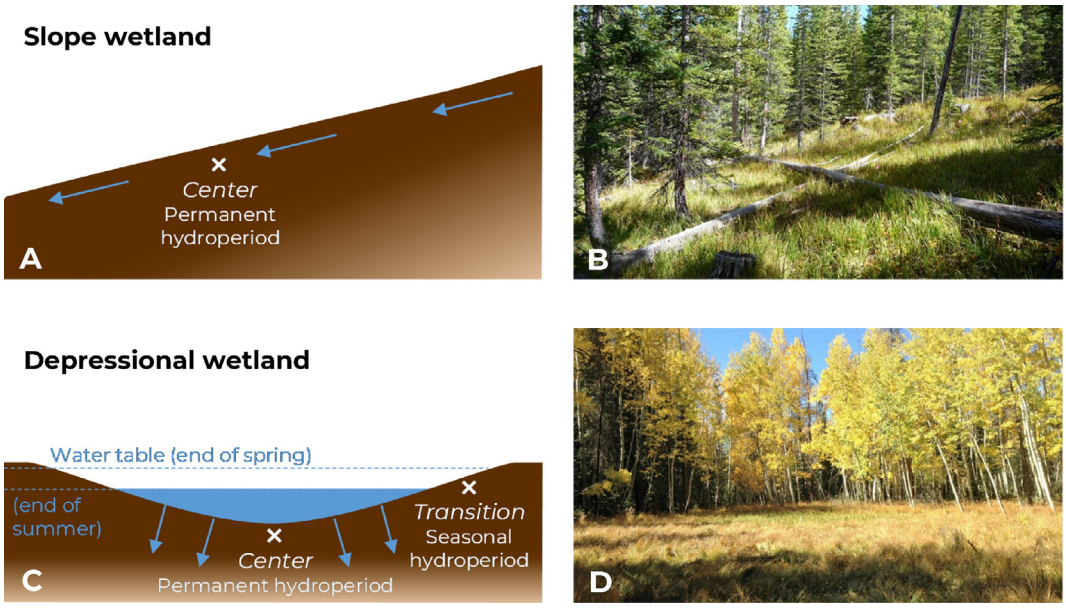

Fig. 1. Schematic diagrams and photographs of the slope (A and B) and depressional (C and D) wetlands showing sampling sites (×). Arrows indicate water movement, and dotted lines indicate water table levels.

a radial inundation gradient: the *center* site is covered in standing water for almost the entire summer, and has a permanent hydroperiod, whereas the peripheral, *transition* site is upslope of the wetland center and has a seasonal hydroperiod, drying down in the late summer months (Fig. 1C and D). Soils of both wetland types are taxonomically described as perennially-saturated Cryofibrists.

Intact soil cores (60–70 cm length, 6 cm diameter) were collected in summer 2015 using a soil corer and slide hammer. All soils were waterlogged at sampling time. Cores were stored anoxically at 4 °C prior to experiments and analyses. We discarded the organic horizon (0–26 cm) and collected undisturbed mineral soil slices (B horizon) from a *shallow* (0–2 cm) depth in the slope wetland and from *shallow* (0–2 cm) and *deep* (40–42 cm) depths in the depressional wetland sites.

2.2. Soil physical and chemical characterization

Soil characteristics were measured for the same depths as those used for the FTR experiments. Soil texture was determined using the hydrometer method (Gee and Or, 2002). Bulk density (D_b) was determined in triplicate after drying a known volume of soil at 105 °C for 24 h. Percent soil OM was determined by weight loss on ignition. Soil pH, cation exchange capacity (CEC), exchangeable acidity (EA), and base saturation (BS) were determined according to standard protocols (Sumner and Miller, 2005; Thomas, 2005). Molar C:N ratio was calculated from total C and total N analyzed by dry combustion on a LECO TruSpec CN analyzer (Leco Corp., St. Joseph, MI, USA; Method Detection Limit (MDL): 0.2%, Analytical Error (AE): 0.02%). Extractable soil boron (B), copper (Cu), Fe, manganese (Mn), phosphorus (P), sulfur (S), zinc (Zn), and aluminum (Al) were analyzed by inductively coupled plasma optical emission spectrometry (SpectroBlue, Spectro Analytical, Kleve, Germany; MDL: 10 µg/L, AE: 3 µg/L) following a Modified Morgan extraction (McIntosh, 1969).

2.3. Flow-through reactor (FTR) experiments

FTRs were assembled according to Pallud et al. (2007). Undisturbed 2 cm long soil slices were packed inside Plexiglas FTR cells (4.2 cm ID, 2 cm L), with both nitrocellulose (0.22 µm) and glass fiber filters (2.7 µm) at each end. The FTRs were sealed with Plexiglas caps. The experiments were conducted in a glove bag under anoxic conditions (4.5% H_2, 95.5% N_2) in a temperature-controlled water bath at either 6 or 18 °C, representing low (e.g. spring/fall) and elevated (e.g. summer) soil temperatures, respectively (Rhoades et al., 2012).

An input solution was supplied to the reactors at a constant volumetric flow rate (1.9 ± 0.3 mL h^{-1}) imposed by a peristaltic pump. This flow rate corresponds to water residence times between 8.6 and 12.1 h mimicking conditions observed for the slope wetland. The input solutions were purged with O_2-free N_2 and contained an average of 0.26 mg Mg^{2+} L^{-1} (as $MgCl_2{\cdot}6H_2O$), 1.17 mg Ca^{2+} L^{-1} (as $CaCl_2{\cdot}2H_2O$), 0.02 mg NH_4^+ L^{-1} (as NH_4Cl), 0.48 mg Na^+ L^{-1} (as $NaHCO_3$), and 0.02 mg K^+ L^{-1} (as K_2HPO_4) to mimic the major chemical composition of the pore-waters in the field (Nelson et al., 2011; Daugherty et al., 2019). Outflow samples were collected every 24 h and analyzed for Fe(II) and DOC. Concentrations of Fe(II) were measured spectrophotometrically at 562 nm with the ferrozine method (Stookey, 1970; MDL: 11 µg/L, AE: 4 µg/L). DOC concentrations were measured using a wet oxidation total inorganic and total organic C analyzer (Model 1010 Wet Oxidation Total Organic/ Total Inorganic Carbon Analyzer OI Analytical, College Station, TX, USA) with reagents 50 g L^{-1} H_3PO_4 for total inorganic

C and 100 g L^{-1} $Na_2S_2O_8$ for total organic C with heat catalysis at 100 °C (MDL: 12 µg/L, AE: 3.5 %).

2.4. Determination of potential Fe(II) and DOC export rates, and apparent temperature coefficient

Potential steady-state Fe(II) and DOC export rates, which represent respectively the fraction of Fe(II) and DOC exported from the soil in the FTR effluent, were calculated following Richards and Pallud (2016) as:

$$Fe(II)\ and\ DOC\ export\ rate = \frac{C_{out}Q}{V} \quad (1)$$

where C_{out} (nmol mL^{-1}) is the Fe(II) or DOC effluent concentrations, Q (mL h^{-1}) is the flow rate, and V (cm^3) is the volume of soil in the FTR. The Fe(II) and DOC export rates are referred to as "potential" because they correspond to conditions when Fe is the predominant terminal electron acceptor available to the soil microbial community. For flow-through reactor experiments, steady-state refers to conditions once the composition of fluid exiting the reactor no longer changes significantly with time (Pallud et al., 2007). Here, Fe(II) and DOC export rates were calculated from data points between 12 and 30 h, and rates are reported as averages of those data points. Fe(II) export rates provide a lower bound for Fe(III) reduction rates due to potential Fe(II) retention through precipitation in secondary mineral products (Pallud et al., 2010), sorption of Fe(II) to clay minerals (Hofstetter et al., 2003), and complexation of Fe(II) with organic molecules sorbed to mineral surfaces (Jansen et al., 2003; Daugherty et al., 2017a).

The cumulated amounts of Fe and DOC lost over the first 30 days of the FTR experiments were calculated from daily Fe(II) and DOC concentrations in the reactor effluent, and the volume eluted *per* day.

Apparent temperature coefficient for Fe(III) reduction, Q_{10}, was calculated following Chen et al. (2014) as:

$$Q_{10} = \left(\frac{R_{18}}{R_6}\right)^{\frac{10}{18-6}} \quad (2)$$

where R_{18} and R_6 are the Fe(II) export rates at 18 and 6 °C.

2.5. Statistical analyses

All statistical tests were conducted using the R programing language (R Core Team, 2016) with a significance threshold of 0.05. Statistical significances of difference in Fe(II) and DOC export rates across study sites, soil depths, and temperatures were determined using a multi-factorial ANOVA followed by Tukey post-hoc HSD. Relationships between Fe(II) and DOC export rates were determined using linear regression.

3. RESULTS

3.1. Soil physical and chemical characteristics

Physical and chemical soil characteristics for the five study mineral soils are shown in Table 1.

All soils were clay-rich, ranging in texture from silty clay loam/silty clay in the slope wetland and depressional center

Table 1
Physical and chemical characteristics of the five study mineral soils.

Wetland type	Depressional	Depressional	Depressional	Depressional	Slope
Location	Center	Center	Transition	Transition	n/a
Depth	*Shallow*[a]	*Deep*[a]	*Shallow*[a]	*Deep*[a]	*Shallow*[a]
Soil characteristics					
Sand content (%)	4.4	12.9	9.8	2.8	4.1
Silt content (%)	58.3	44.2	31.6	34.9	59.3
Clay content (%)	37.3	43.0	58.6	62.2	36.6
Textural class	Silty clay loam	Silty clay	Clay	Clay	Silty clay loam
Dry bulk density (g cm^{-3})	0.36	0.31	0.31	0.42	0.83
pH	4.8	5.1	4.1	4.6	5.6
Cation exchange capacity (meq 100 g^{-1})	34.9	36.9	32.5	32.7	34.7
Exchangeable acidity (meq 100 g^{-1})	14.1	15.3	22.0	20.4	13.7
Base saturation (%)	59.7	58.4	32.3	37.8	60.6
Organic matter content (%)	30.5	18.3	42.8	13.9	12.9
Molar C_{org}:N ratio	11.8	19.5	13.6	18.7	18.6
Total N content (%)	0.92	0.88	1.4	0.75	0.08
C_{org} content (%)	17.5 ± 3.6[b]	10.8 ± 2.6[b]	20.8 ± 5.6[b]	7.3 ± 1.3[b]	4.7 ± 2.0[b]
Extractable B content (nmol g^{-1})	8.8	bdl	34.3	bdl	bdl
Extractable Cu content (nmol g^{-1})	4.7	1.5	6.6	bdl	1.9
Extractable Fe content (µmol g^{-1})	3.2	1.8	2.9	0.86	0.53
Extractable Mn content (µmol g^{-1})	0.13	0.35	0.08	0.15	0.68
Extractable P content (nmol g^{-1})	32.0	7.0	39.3	4.4	8.2
Extractable S content (µmol g^{-1})	1.48	0.91	0.97	0.36	0.82
Extractable Zn content (nmol g^{-1})	19.9	4.5	8.0	bdl	2.3
Extractable Al content (µmol g^{-1})	3.5	1.5	13.0	3.3	0.66

bdl: below detection limits.
[a] *Shallow* refers to the depth 0–2 cm and *deep* refers to the depth 40–42 cm in the mineral soil.
[b] Average and standard deviation from 5 cores.

sites to clay in the depressional transition site. Clay contents ranged from 37.3% to 62.2% and increased marginally with depth in both the depressional wetland sites. All study soils were acidic, with pH ranging from 4.1 to 5.6, and had high OM content (12.9–42.8%). Reflecting their high OM content, all soils had a low dry bulk density, with values of 0.31–0.42 for the four depressional wetland soils, and a value twice higher (0.83) in the slope wetland soil. Overall, molar C:N ratios ranged between 11.8 and 19.5, were about 1.5 times higher in the slope wetland soils than in the depressional wetland soils, and increased with depth by a factor of 1.5.

Within the depressional wetland, the concentrations of OM, Fe and all other nutrients, except Mn, decreased with depth (Table 1). The slope wetland soils had lower concentrations of OM, Al and all tested nutrients, except Mn, than the depressional wetland soils (Table 1). For example, for similar depths, the slope wetland soil had 12–18, 5–6 and 4–5 times less N, Fe, and P, respectively, but 5–9 times more extractable Mn than the depressional wetland soils.

3.2. Fe(II) export rates

Fe(II) concentrations in the reactor effluent varied with study sites, soil depths, and incubation temperatures (Fig. A.1, 2) and ranged between below detection limit and 82 μM at 6 °C and between below detection limit and 202 μM at 18 °C. For the FTR experiments performed at 18 °C in all shallow soils, Fe(II) was detected in the effluent immediately and the effluent Fe(II) concentrations reached a steady-state after 11–30 days (21–126 pore volumes) (Fig. A.1). Concentrations detected on day 1 were higher than 150 μM in the two shallow soils of the depressional wetland, but lower than 32 μM in the other three soils. For most of the FTR experiments performed at 6 °C, Fe (II) export was delayed. Fe(II) export was very limited in the deep depressional wetland soils, where Fe(II) was detected at much lower concentrations than all other soils, with most values below detection limit (Fig. A.1B and D). Cumulated soil Fe loss ranged from 3.5 to 35.6% of the original pool. For both temperatures, the cumulated Fe export was 2–9 times higher in the two shallow soils of the depressional wetland than in the three other soils (Fig. A.1F).

Analysis of variance indicated that incubation temperatures, study sites, and soil depths interacted to significantly affect Fe(II) export rate ($p \leq 0.001$, Fig. 2). Across all sites, Fe(II) export rates were on average 57% lower ($p \leq 0.001$) at 6 °C than at 18 °C (Fig. 3). More specifically, higher temperature led to significantly higher Fe(II) export rates in the four depressional wetland soils, with mean Fe(II) export rates ranging between 0.5 and 5.9 nmol cm^{-3} h^{-1} at 18 °C compared to 0.2 and 3.4 nmol cm^{-3} h^{-1} at 6 °C (Fig. 2), leading to Fe(II) export rates that were on average 84.8% lower ($p \leq 0.001$) at 6 °C than at 18 °C (data not shown). At 18 °C, mean Fe(II) export rates were the highest in the two shallow depressional wetland soils, being 3–11 times higher than in the three other soils at the same temperature. At 6 °C, mean Fe(II) export rates were 10–17 times lower for the two deep soils of the depressional wetland than in the three other soils, which did not show any significant difference among them. For both temperatures, the lowest mean Fe(II) export rates were found in the deep soils of the depressional wetland (Fig. 2). With very few exceptions, the effluent pH did not change drastically over time once steady-state was reached for Fe(II) and DOC concentrations (Fig. A.2). For those time points, effluent pH for the depressional center site averaged 5.2 ± 0.1 (6 °C) and

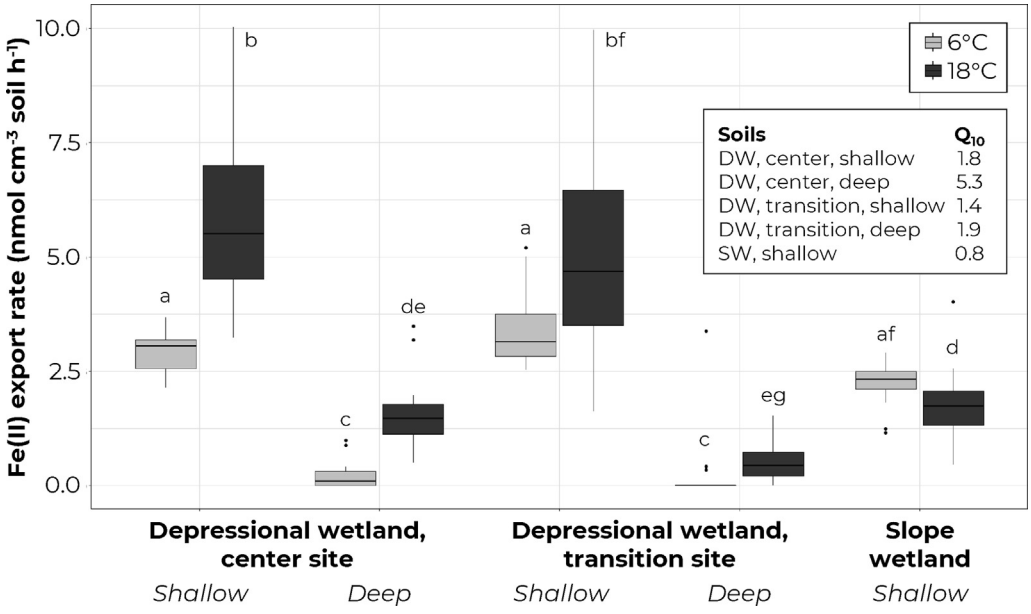

Fig. 2. Median Fe(II) export rates with standard error bars calculated from continuous flow-through reactor experiments performed on intact soil cores at 6 °C (light grey) and 18 °C (dark grey). Different letters denote significant differences ($p > 0.05$) among sites, depths and temperature combinations. Table summarizes Q_{10} for all soils, with DW and SW indicating depressional and slope wetlands.

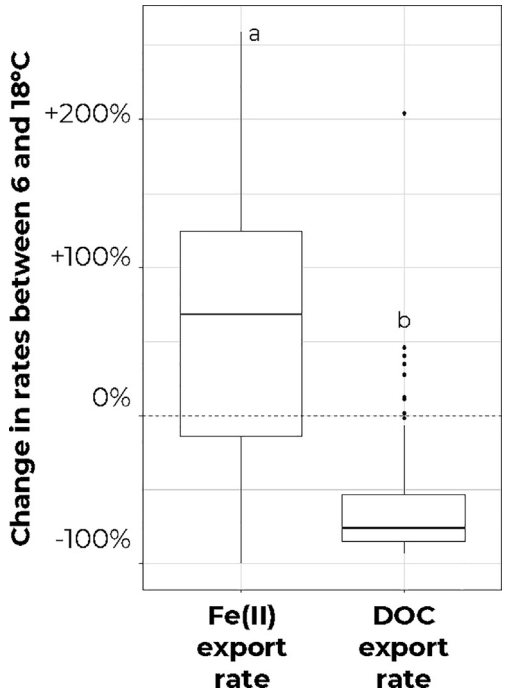

Fig. 3. Change in Fe(II) and DOC export rates between 6 and 18 °C, averaged across all sites and depths. Different letters indicate significant differences ($p < 0.001$).

6.2 ± 0.2 (18 °C) and 5.1 ± 0.1 (6 °C) and 5.9 ± 0.3 (18 °C) for shallow and deep depths, respectively. Effluent pH for the depressional transition site averaged 5.2 ± 0.1 (6 °C) and 5.4 ± 0.1 (18 °C) and 5.0 ± 0.2 (6 °C) and 4.9 ± 0.1 (18 °C) for shallow and deep depths, respectively. Effluent pH in the shallow slope wetland soil averaged 6.2 ± 0.3 (6 °C) and 6.3 ± 0.3 (18 °C). Although not significant, there was a tendency for higher Fe(II) export from soils with higher OM, N, extractable P, Fe, Zn, B, and Cu, but lower extractable Mn and C:N ratio, especially at 18 °C (Fig. 4). At 6 °C, the same tendency was observed (Fig. A.3), however the slope wetland behaves differently. We suspect that these differences reflect distinct microbial community composition in the two wetland types. Neither soil physical properties or pH influenced Fe(II) export at either temperature. Regression analyses found no relation between Fe(II) export rate and effluent pH across wetland sites and depths.

3.3. DOC export rates

DOC concentrations in the reactor effluent, and consequently, DOC export rates, varied between study sites and incubation temperatures, but were not affected by soil depth (Fig. A.4, 5). DOC concentrations ranged between 0.4 and 6.3 μM at 6 °C and between below detection limit and 5.8 μM at 18 °C. For all soils and incubation temperatures, unbound DOC was flushed out of the soil at the beginning of the experiments, resulting in DOC being detected in the effluent at the first sampling point at concentrations ranging between below 1.8 and 3.7 μM at 6 °C and between 3.1 and 5.8 μM at 18 °C (Fig. A.4). For all FTR experiments performed at 18 °C, DOC breakthrough curves were similar and effluent DOC concentrations reached a steady-state after 10 days (19–42 pore volumes). For FTR experiments performed at 6 °C, effluent DOC concentrations also reached a steady-state after 10 days, but DOC concentrations increased again and reached a new steady-state after 24 days for the transition site of the depressional wetland and the slope wetland. The cumulated DOC loss was equivalent to a 0.03–1.4% decrease in soil C stock (data not shown), and was 2 to 8 times higher at 6 °C than at 18 °C (Fig. A.4F). For both temperatures, the lowest cumulated DOC loss was observed in the shallow soil of the slope wetland (Fig. A.4F).

Across all sites, DOC export rates were 60% higher ($p \leq 0.001$) at 6 °C than at 18 °C (Fig. 3), where they were equal among all study soils (Fig. 5). More specifically, mean DOC export rates ranged between 96.2 and 168.6 nmol cm^{-3} h^{-1} at 6 °C and between 25.9 and 49.4 nmol cm^{-3} h^{-1} at 18 °C (Fig. 5). The DOC export rates obtained at 6 °C varied significantly between the three study sites with the highest rates observed in the depressional wetland center site and the lowest rates observed in the slope wetland site (Fig. 5). There was no correlation between DOC export rates and any of the measured soil characteristics.

Fe(II) and DOC export rates were positively correlated in the shallow soils of the depressional wetland at both incubation temperatures (Fig. 6). There was a stronger association between the two at 6 °C than at 18 °C, with regression line slopes an order of magnitude higher at the lower temperature. No correlation was observed between Fe(II) and DOC export rates in the slope wetland soil, or for the deep soils, regardless of incubation temperature (data not shown). Similar to Fe(II) export, there was no relation between DOC export rate and effluent pH across sites and depths.

4. DISCUSSION

4.1. Soil characteristic influencing potential Fe(II) export rates

Our results showed that the reductive dissolution rates of Fe(III)-bearing minerals in subalpine wetland soils could be influenced by C substrate quantity and quality (i.e., molar C:N ratio), the availability of nutrients, and the relative availability of the terminal electron acceptors Fe and Mn. Indeed, at 18 °C, the two soils which exhibit the highest Fe(II) export rates, used as lower bound proxies for Fe (III) reduction rates, have the highest extractable Fe substrate content, the highest levels of macro- and micronutrients, except Mn, the highest OM content, and C:N ratios closest to 10, the optimum for heterotrophic bacterial respiration (Fenchel et al., 2012). This corroborates previous observations that reductive dissolution of ferrihydrite and goethite is the highest in the presence of OM with relatively low C:N (e.g., 9.7) (Petruzzelli et al., 2005), indicating that Fe(III)-reducing microorganisms depend on soil OM that supplies both N and C.

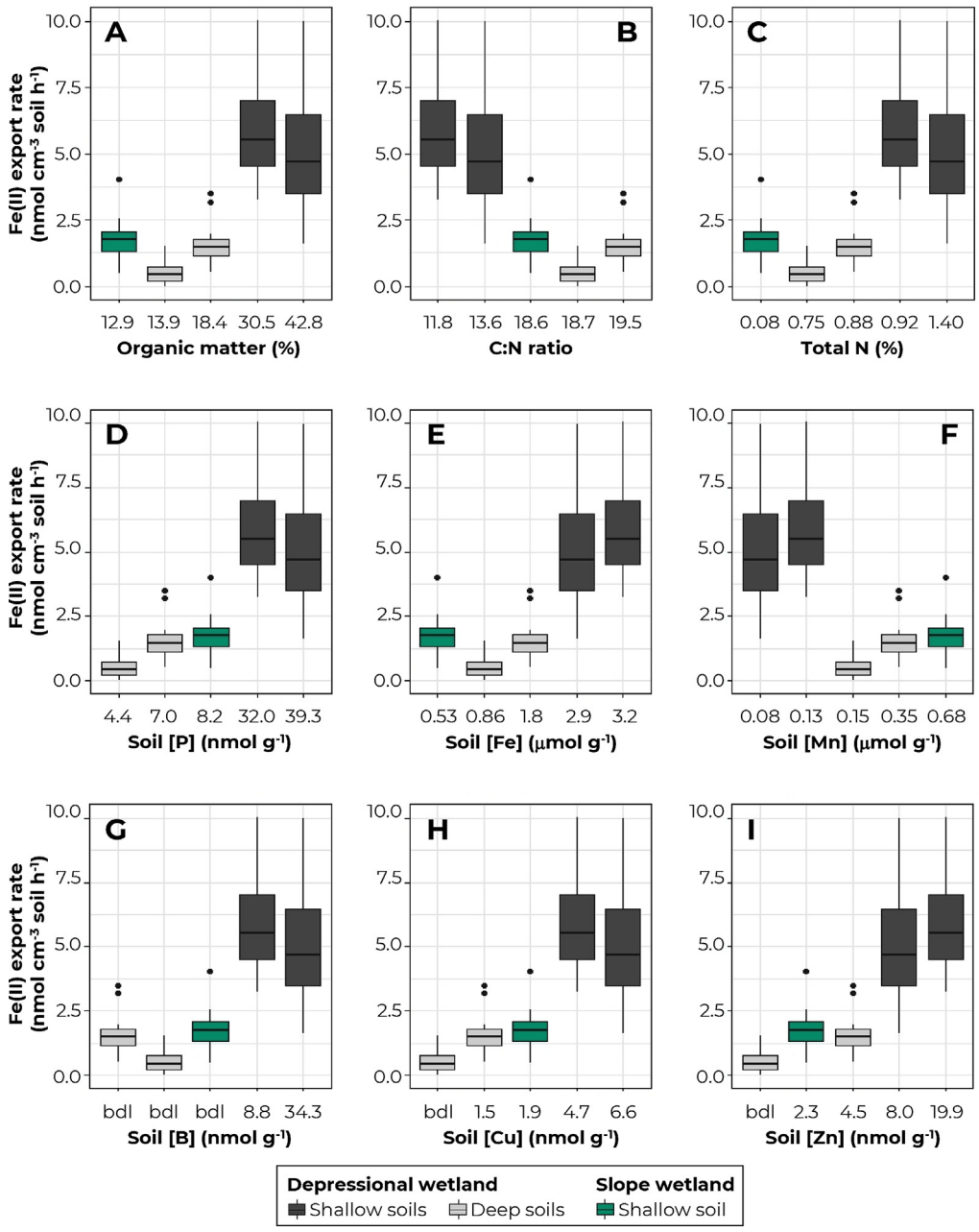

Fig. 4. Relationships between Fe(II) export rates at 18 °C and selected soil chemical characteristics for shallow (dark grey) and deep soils (light grey) of the depressional wetland, and for shallow soils of the slope wetland (green). No trend was observed with soil physical properties or pH, so they were omitted. bdl: below detection limits. (For interpretation of the references to color in this figure legend, the reader is referred to the web version of this article.)

The inverse trend between Fe(II) export and extractable Mn concentrations (Fig. 4) could reflect the exclusion of microbial Fe(III)-reducing activities by more energetically favorable Mn-oxides as terminal electron acceptors, and/or the abiotic oxidation of Fe(II) by Mn-oxides (Borch and Kretzschmar, 2010; Melton et al., 2014); both processes have been observed in tundra wet meadow soils where genetic sequence data identified the presence of microbial taxa typically found in wetlands (Costello and Schmidt, 2006). However, inhibition of Fe(III) reduction by the presence of Mn is unlikely to occur in our organic-rich study soils, which probably allows dissimilatory Fe(III) and Mn (IV) reduction to co-occur as C substrate availability is not limiting (Lovley, 1991; Urban et al., 1994; Paul et al., 2006). Therefore abiotic oxidation of microbially-produced Fe(II) by Mn(IV, III)-oxides more likely plays a role in the slope wetland's low Fe(II) export rates. Additionally, we measured a much smaller pool of highly reactive Fe in the slope wetland soil (Table 2), despite its 5–10 times higher concentration of HCl-extracted Fe compared

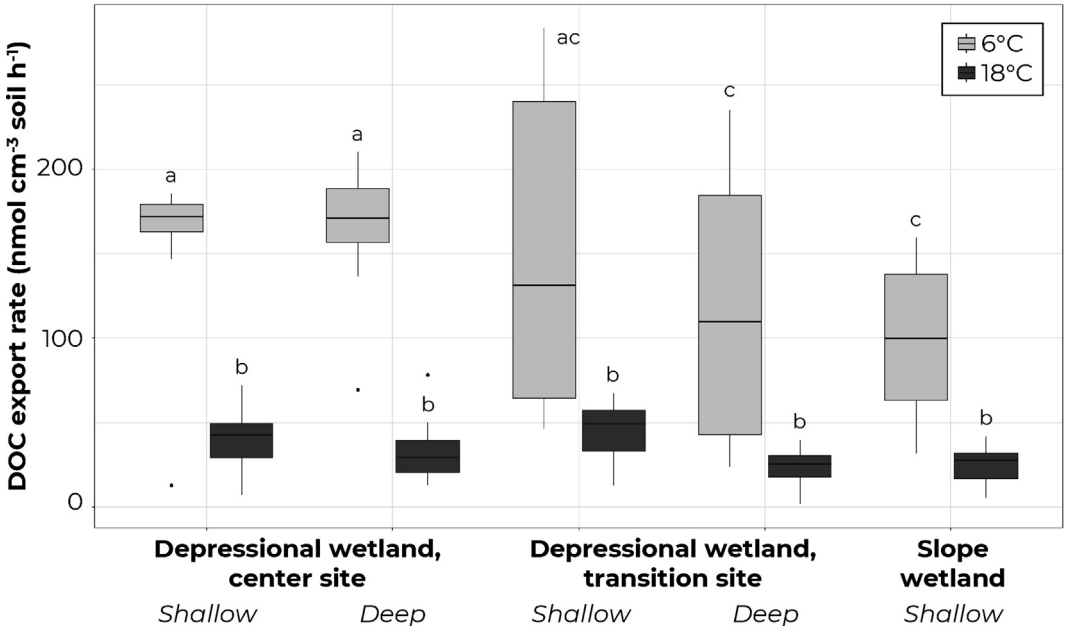

Fig. 5. Median DOC export rates with standard error bars calculated from continuous flow-through reactor experiments performed on intact soil cores at 6 °C (light grey) and 18 °C (dark grey). Different letters denote significant differences ($p > 0.05$) among sites, depths and temperature combinations.

to the depressional wetland soils (Schilling et al., 2019). This further indicates that low availability of Fe phases probably limits Fe(II) export from the slope wetland soil. Chemical or microbial oxidation of Fe(II) by O_2 (Melton et al., 2014), as well as anaerobic Fe(II) oxidation by phototrophic or nitrate-reducing microorganisms (Peng et al., 2018; Peng et al., 2019) are unlikely to occur in our systems due to the lack of O_2, light and nitrate in these wetland soils (Daugherty et al., 2019). We did not observe any effect of soil physical properties or soil pH on Fe(II) export rates, however, it does not mean that such an effect does not exist, but it most likely reflects the limited range of those properties in our study soils.

4.2. Temperature response of Fe(II) and DOC export rates

We observed that both Fe and C cycling were temperature-sensitive in these wetland soils. Indeed, Fe(II) export rates were 84.8% higher at 18 °C than at 6 °C in the four depressional wetland soils, and DOC export rates were 60.0% lower at 18 °C than at 6 °C in all study soils.

Recent field studies have suggested the following mechanisms to explain warming-related decreases in DOC concentrations: (a) increased sorption of DOC due to exposure of new mineral surfaces by thawing (Frey and McClelland, 2009), (b) increased microbial access to DOC due to decreased flow velocities (Grosse et al., 2011; Striegl et al., 2012), and (c) increased microbial processing of DOC due to increased microbial activity with temperature (Striegl et al., 2005, 2012). Neither mineral surface exposure nor flow velocity varied in our experiments, which leaves enhanced microbial consumption of DOC (mechanism c), as the most likely explanation for our results. This is supported by field observations of increased CO_2 soil efflux in our study wetlands with seasonal temperature increases (Daugherty et al., 2019). This mechanism is also strongly supported by lower soil C remaining after incubation at 18 °C than at 6 °C (Table 2). Even if more DOC is released at higher temperature due to higher Fe(III) reduction rates, higher C consumption resulting from stimulated microbial activity caused a net decline in DOC concentrations. Similar conclusions have been drawn from laboratory experiments using intact peat soil cores (Clark et al., 2009) as well as from large basin scale modeling of a permafrost-dominated watershed (Striegl et al., 2005). Higher DOC sorption in mineral soils has been observed with increased temperature (10–23 °C range, Jardine et al., 1989; 7 to 45 °C range, Daugherty et al., 2017b) indicating that increased sorption capacity may be partially responsible for the lower DOC loss observed here at 18 °C.

4.3. Implications for in situ Fe(III) and DOC cycling in wetland soils

Our data suggest that *in situ* Fe(III) reduction rates could increase in response to seasonal temperature increases spanning weeks or months. A previous study in these same wetland soils found that Fe(III) reduction was temperature-sensitive when soluble-Fe(III) was supplied as the sole terminal electron acceptor with Q_{10} values of 1.5–4.2 (Schilling et al., 2019). Here, we found the Q_{10} of Fe(II) export rate ranged from 0.8 to 5.3 with a mean of 2.2 (Fig. 2). In the absence of comparable wetland studies, we compare our findings to the best-available natural environment. Our Q_{10} values are similar to those for Fe(III) reduction in acidic lake sediments supplied with synthetic Fe(III)-oxyhydroxide (1.8–2.0, Meier et al., 2005) or sediments of a eutrophic lake (1.19–3.54, Chen et al., 2014)

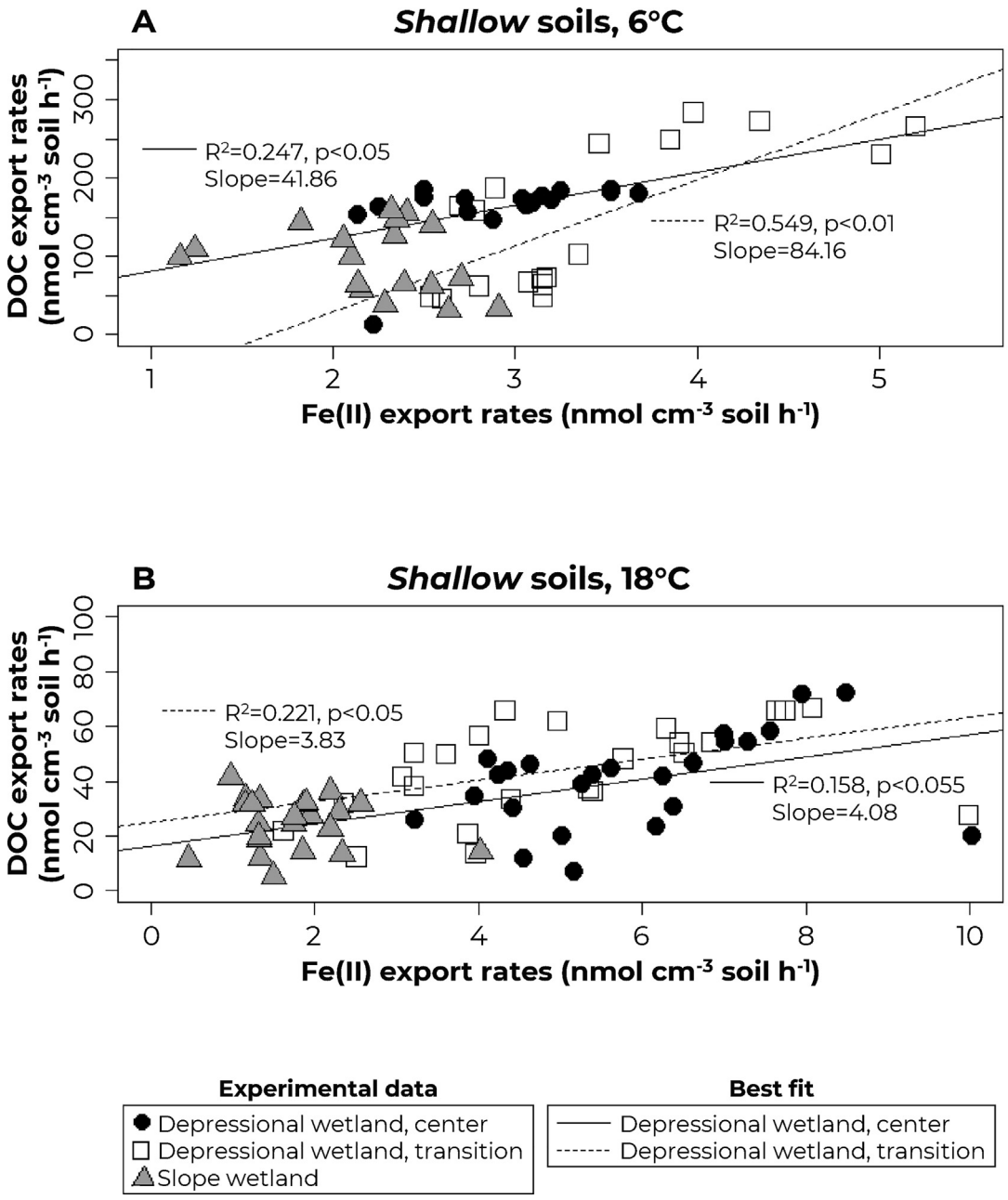

Fig. 6. Least squares regression of DOC export rates as a function of Fe(II) export rates for shallow soils of the depressional wetland *center* site (black circles), the depressional wetland *transition* site (white squares), and the slope wetland site (grey triangles) at 6 °C (A) and 18 °C (B). When the best linear fit is significant ($p \leq 0.05$) the regression line, correlation coefficient (R^2), and significance values are given. No correlation was observed between Fe(II) and DOC export rates for the deep soils, so they were omitted.

and are consistent with microbial communities that are well adapted to low temperature environments.

However, we show that DOC export could decrease in response to seasonal temperature increases. This is the likely outcome of greater microbial activity and C mineralization at higher temperatures and is consistent with seasonal patterns in stream DOC export in surrounding watersheds (Rhoades et al., 2017). Future work should determine temperature effects on DOC sorption to iron-rich mineral soil, measure CO_2 losses during Fe(III) reduction, and include an evaluation of the biogeochemical reactivity of DOC in order to determine the potential implications for global C cycling.

Our data show that the susceptibility of wetlands to temperature-related changes in Fe-C dynamics varies among wetland types and among soil depths associated with their organic content and chemical characteristics, especially their bioavailable Fe content. As such, with seasonal temperature increases, we expect increases in microbial Fe(III) respiration and associated CO_2 production

Table 2
Soil carbon content at termination of flow-through experiments at 6 and 18 °C. Values are reported as average ± standard deviation for analyses on triplicate samples.

	Final soil C content (%) 6 °C	Final soil C content (%) 18 °C
Depressional wetland, center, *shallow*	17.8 ± 0.11	13.7 ± 0.08
Depressional wetland, center, *deep*	14.4 ± 0.79	12.4 ± 0.20
Depressional wetland, transition, *shallow*	24.4 ± 0.33	19.8 ± 0.03
Depressional wetland, transition, *deep*	7.4 ± 0.15	6.0 ± 0.06
Slope wetland, *shallow*	4.8 ± 0.24	2.3 ± 0.16

(Roden and Wetzel, 1996; Lipson et al., 2010; Lipson et al., 2013) and soil C losses from soils to pore-water in the soils of the depressional wetlands. Increased Fe(III) respiration has the potential to decrease soil C stocks because reduction dissolution of Fe(III)-oxyhydroxides will release coprecipitated and adsorbed DOC and through enhanced microbial consumption of the DOC by Fe(III)-reducers (Striegl et al., 2005; Dutta et al., 2006; Gutierrez and Jones, 2006; Hartley et al., 2008; Clark et al., 2009; Wallenstein and Hall, 2012; Karhu et al., 2014). Shallow depressional wetland soils contain the highest C stocks of our study soils, and may be susceptible to the greatest temperature-related changes. The molar C:N ratio of these soils is near-optimal for microbial respiration, and there is periodic re-generation of Fe(III) during seasonal redox changes (Knorr, 2013; Ginn et al., 2017; Barcellos et al., 2018). The Fe(III) reduction rates are likely to be less responsive to increased temperatures in the slope wetland soils, as they are constantly inundated with cold, emergent groundwater that dampens temperature fluctuations (Wallenstein and Hall, 2012; Mills et al., 2014). Furthermore, Fe(II) reduction is likely limited in the slope wetland soils, due to the presence of dissolved oxygen in porewaters and to limited redox fluctuations, which lead to more thermodynamically stable Fe-oxides. Thus, future carbon cycling models need to consider wetland type, Fe reduction potential and soil temperature when estimating DOC release from soils to porewaters and from porewaters to surface water.

Declaration of Competing Interest

The authors declare that they have no known competing financial interests or personal relationships that could have appeared to influence the work reported in this paper.

ACKNOWLEDGEMENTS

The authors thank H. Barnhart, E. Daugherty, C. Fossum, J. Gomez, S. Matzen, C. Richards, K. Schilling, M. Welch-Siegel, and N. Zhang for their help in the field and laboratory. This project was supported by USDA-NIFA Grant no. 2013-67019-21359. Additional funding was provided by the Esper Larsen Jr. Fund, the Bay Area Water Quality Fellowship, CMS, UCOP Carbon Neutrality Initiative, and the SSSA Wetlands Division.

APPENDIX A. SUPPLEMENTARY MATERIAL

Supplementary data to this article can be found online at https://doi.org/10.1016/j.gca.2020.03.023.

REFERENCES

Ameli A. A. and Creed I. F. (2017) Quantifying hydrologic connectivity of wetlands to surface water systems. *Hydrol. Earth Syst. Sci.* **21**, 1791–1808.

Amstaetter K., Borch T. and Kappler A. (2012) Influence of humic acid imposed changes of ferrihydrite aggregation on microbial Fe(III) reduction. *Geochim. Cosmochim. Acta* **44**, 326–341.

Barcellos D., Cyle K. T. and Thompson A. (2018) Faster redox fluctuations can lead to higher iron reduction rates in humid forest soils. *Biogeochemistry* **137**, 367–378.

Barnett T. P., Adam J. C. and Lettenmaier D. P. (2005) Potential impacts of a warming climate on water availability in snow-dominated regions. *Nature* **438**, 303–309.

Bernal B. and Mitsch W. J. (2012) Comparing carbon sequestration in temperate freshwater wetland communities. *Global Change Biol.* **18**, 1636–1647.

Björnerås C., Weyhenmeyer G. A., Evans C. D., Gessner M. O., Grossart H.-P., Kangur K. and Kritzberg E. S. (2017) Widespread increases in iron concentration in European and North American freshwaters. *Global Biogeochem. Cycles* **31**, 1488–1500.

Borch T. and Kretzschmar R. (2010) Biogeochemical redox processes and their impact on contaminant dynamics. *Environ. Sci. Technol.* **44**, 15–23.

Brinson M. M. (1993) A Hydrogeomorphic Classification for Wetlands. U.S. Army Engineer Waterways Experiment Station, Vicksburg, Miss.

Carnell P. E., Windecker S. M., Brenker M., Baldock J., Masque P., Brunt K. and Macreadi P. I. (2018) Carbon stocks, sequestration, and emissions of wetlands in south eastern Australia. *Global Change Biol.* **24**, 4173–4184.

Chen M., Ye T.-R., Krumholz L. R. and Jian H.-L. (2014) Temperature and cyanobacterial bloom biomass influence phosphorous cycling in eutrophic lake sediments. *PLOS* **9**, 1–10.

Clark J. M., Ashley D., Wagner M., Chapman P. J., Lane S. N., Evans C. D. and Heathwaite A. L. (2009) Increased temperature sensitivity of net DOC production from ombrotrophic peat due to water table draw-down. *Global Change Biol.* **15**, 794–807.

Clark J. M., Bottrell S. H., Evans C. D., Monteith D. T., Bartlett R., Rose R., Newton R. J. and Chapman P. J. (2010) The importance of the relationship between scale and process in understanding long-term DOC dynamics. *Sci. Total Environ.* **408**, 2768–2775.

Costello E. K. and Schmidt S. K. (2006) Microbial diversity in alpine tundra wet meadow soil: novel Chloroflexi from a cold, water-saturated environment. *Environ. Microbiol.* **8**, 1471–1486.

Covino T. (2017) Hydrologic connectivity as a framework for understanding biogeochemical flux through watersheds and along fluvial networks. *Geomorphology* **277**, 133–144.

Daugherty E. E., Gilbert B., Nico P. S. and Borch T. (2017) Complexation and redox buffering of iron(II) by dissolved organic matter. *Environ. Sci. Technol.* **51**, 11096–11104.

Daugherty E., Lobo G., Pallud C. E. and Borch T. (2017b) Temperature and chemical composition controls on sorption of DOC to iron hydroxides under dynamic flow conditions. American Geophysical Union, Fall Meeting 2017. #B21J-07 (abstract).

Daugherty E. E., McKee G. A., Bergstrom R., Burton S., Pallud C., Hubbard R. M., Kelly E. F., Rhoades C. C. and Borch T. (2019) Hydrogeomorphhic controls on soil carbon composition in two classes of subalpine wetlands. *Biogeochem.* **145**, 161–175.

Dutta K., Schuur E. A. G., Neff J. and Zimov S. A. (2006) Potential carbon release from permafrost soils of Northeastern Siberia. *Global Change Biol.* **12**, 2336–2351.

Emsens W.-J., Aggenbach C. J. S., Schouten K., Smolder A. J. P., Zak D. and van Diggelen R. (2016) Soil iron content as a predictor of carbon and nutrient mobilization in rewetted fens. *PLoS One* **11**(4) e0153166.

Eusterhues K., Hadrich A., Neidhardt J., Kusel K., Keller T. F., Jandt K. D. and Totsche K. U. (2014) Reduction of ferrihydrite with adsorbed and coprecipitated organic matter: microbial reduction by *Geobacter bremensis* vs. abiotic reduction by Na-dithionite. *Biogeosciences* **11**, 4953–4966.

Evans C. D., Freeman C., Monteith D. T., Reynolds B. and Fenner N. (2002) Terrestrial export of organic carbon - Reply. *Nature* **415**, 862.

Evans C. D., Monteith D. T. and Cooper D. M. (2005) Long-term increases in surface water dissolved organic carbon: observations, possible causes and environmental impacts. *Environ. Poll.* **137**, 55–71.

Evans C. D., Chapman P. J., Clark J. M., Monteith D. T. and Cresser M. S. (2006) Alternative explanations for rising dissolved organic carbon export from organic soils. *Global Change Biol.* **12**, 2044–2053.

Fenchel T., King G. and Blackburn H. (2012) *Bacterial Biogeochemistry: The Ecophysiology of Mineral Cycling*. Academic Press, San Diego, USA.

Findlay S. (2005) Increased carbon transport in the Hudson River: unexpected consequence of nitrogen deposition? *Front. Ecol. Environ.* **3**, 133–137.

Freeman C., Evans C. D., Monteith D. T., Reynolds B. and Fenner N. (2001) Export of organic carbon from peat soils. *Nature* **412**, 785.

Freeman C., Fenner N., Ostle N. J., Kang H., Dowrick D. J., Reynolds B., Lock M. A., Sleep D., Hughes S. and Hudson J. (2004) Export of dissolved organic carbon from peatlands under elevated carbon dioxide levels. *Nature* **430**, 195–198.

Frey K. E. and McClelland J. W. (2009) Impacts of permafrost degradation on arctic river biogeochemistry. *Hydrol. Process.* **23**, 169–182.

Gee G. and Or D. (2002) Particle-size analysis. In *Methods of Soil Analysis, Part 4 Physical Methods* (eds. J. H. Dane and G. C. Topp). Soil Science Society of America, Madison, pp. 255–293.

Ginn B., Meile C., Wilmoth J., Tang Y. and Thompson A. (2017) Rapid iron reduction rates are stimulated by high-amplitude redox fluctuations in a tropical forest soil. *Environ. Sci. Technol.* **51**, 3250–3259.

Grosse G., Harden J., Turetsky M., McGuire A. D., Camill P., Tarnocai C., Frolking S., Schuur E. A. G., Jorgenson T., Marchenko S., Romanovsky V., Wickland K. P., French N., Waldrop M., Bourgeau-Chavez L. and Striegl R. G. (2011) Vulnerability of high-latitude soil organic carbon in North America to disturbance. *J. Geophys. Res. Biogeosciences* **116**, 1–23.

Grybos M., Davranche M., Gruau G. and Petitjean P. (2007) Is trace metal release in wetland soils controlled by organic matter mobility or Fe-oxyhydroxides reduction? *J. Colloid Interface Sci.* **314**, 490–501.

Grybos M., Davranche M., Gruau G., Petijean P. and Pédrot M. (2009) Increasing pH drives organic matter solubilization from wetland soils under reducing conditions. *Geoderma* **154**, 13–19.

Gu B., Schmitt J., Chen Z., Liang L. and McCarthy J. F. (1994) Adsorption and desorption of natural organic matter on iron oxide: mechanisms and models. *Environ. Sci. Technol.* **28**, 38–46.

Gutierrez J. L. and Jones C. G. (2006) Physical ecosystem engineers as agents of biogeochemical heterogeneity. *Bioscience* **56**, 227.

Hartley I. P., Hopkins D. W., Garnett M. H., Sommerkorn M. and Wookey P. A. (2008) Soil microbial respiration in arctic soil does not acclimate to temperature. *Ecol. Lett.* **11**, 1092–1100.

Hemond H. F. (1990) Wetlands as the source of dissolved organic carbon to surface waters. In *Organic Acids in Aquatic Ecosystems* (eds. E. M. Perdue and E. T. Gjessing). John Wiley & Sons, New York, pp. 301–313.

Herndon E. M., Yang Z., Bargar J., Janot N., Regier T. Z., Graham D. E., Wullschleger S. D., Gu B. and Liang L. (2015) Geochemical drivers of organic matter decomposition in arctic tundra soil. *Biogeochemistry* **126**, 397–414.

Herndon E., AlBashaireh A., Singer D., Chowdhury T. R., Gu B. and Graham D. (2017) Influence of iron redox cycling on organo-mineral associations in Arctic tundra soil. *Geochim. Cosmochim. Acta* **207**, 210–231.

Hinton M. J., Schiff S. L. and English M. C. (1998) Sources and flowpaths of dissolved organic carbon during storms in two forested watersheds of the Precambrian Shield. *Biogeochemistry* **41**, 175–197.

Hofstetter T. B., Schwarzenbach R. P. and Haderlein S. B. (2003) Reactivity of Fe(II) species associated with clay minerals. *Environ. Sci. Technol.* **37**, 519–528.

Jansen B., Nierop K. G. J. and Verstraten J. M. (2003) Mobility of Fe(II), Fe(III) and Al in acidic forest soils mediated by dissolved organic matter: influence of solution pH and metal/organic carbon ratios. *Geoderma* **113**, 323–340.

Jardine P. M., Weber N. L. and McCarthy J. F. (1989) Mechanisms of dissolved organic-carbon adsorption on soil. *Soil Sci. Soc. Am. J.* **53**, 1378–1385.

Kaiser K. and Guggenberger G. (2007) Sorptive stabilization of organic matter by microporous goethite: sorption into small pores vs. surface complexation. *Eur. J. Soil Sci.* **58**, 45–59.

Karhu K., Auffret M. D., Dungait J. A., Hopkins D. W., Prosser J. I., Singh B. K., Subke J., Wookey P. A., Ågren G. I., Sebastià M., Gouriveau F., Bergkvist G., Meir P., Nottingham A. T., Salinas N. and Hartley I. P. (2014) Temperature sensitivity of soil respiration rates enhanced by microbial community response. *Nature* **513**, 81–84.

Knorr K. H. (2013) DOC-dynamics in a small headwater catchment as driven by redox fluctuations and hydrological flow paths - Are DOC exports mediated by iron reduction/oxidation cycles? *Biogeosciences* **10**, 891–904.

Knorr K., Lischeid G. and Blodau C. (2009) Dynamics of redox processes in a minerotrophic fen exposed to a water table manipulation. *Geoderma* **153**, 379–392.

Kritzberg E. S. and Ekström S. M. (2012) Increasing iron concentrations in surface waters - A factor behind brownification? *Biogeosciences* **9**, 1465–1478.

Lalonde K., Mucci A., Ouellet A. and Gelinas Y. (2012) Preservation of organic matter in sediments promoted by iron. *Nature* **483**, 198–200.

Lipson D. A., Jha M., Raab T. K. and Oechel W. C. (2010) Reduction of iron (III) and humic substances plays a major role in anaerobic respiration in an Arctic peat soil. *J. Geophys. Res. Biogeo.* **115**, G00I06.

Lipson D. A., Raab T. K., Goria D. and Zlamal J. (2013) The contribution of Fe (III) and humic acid reduction to ecosystem

respiration in drained thaw lake basins of the Arctic Coastal Plain. *Global Biogeochem. Cycles* **27**, 399–409.
Lovley D. R. (1991) Dissimilatory Fe(III) and Mn(IV) reduction. *Microbiol. Rev.* **55**, 259–287.
Maltby E. and Barker T. (2009) *The Wetlands Handbook*. Wiley-Blackwell, West Sussex, UK.
McIntosh J. L. (1969) Bray and Morgan soil test extractants modified for testing acid soils from different parent materials. *Agron. J.* **61**, 259–265.
Meier J., Costa R., Smalla K., Boehrer B. and Wendt-Potthoff K. (2005) Temperature dependence of Fe(III) and sulfate reduction rates and its effect on growth and composition of bacterial enrichments from an acidic pit lake neutralization experiment. *Geobiology* **3**, 261–274.
Mejia J., He S., Yang Y., Ginder-Vogel M. and Roden E. E. (2018) Stability of ferrihydrite–humic acid coprecipitates under iron-reducing conditions. *Environ. Sci. Technol.* **52**, 13174–13183.
Melton E. D., Swanner E. D., Behrens S., Schmidt C. and Kappler A. (2014) The interplay of microbially mediated and abiotic reactions in the biogeochemical Fe cycle. *Nat. Rev. Microbiol.* **12**, 797–808.
Mills R. T. E., Gavazov K. S., Spiegelberger T., Johnson D. and Buttler A. (2014) Diminished soil functions occur under simulated climate change in a sup-alpine pasture, but heterotrophic temperature sensitivity indicates microbial resilience. *Sci. Total Environ.* **473–474**, 465–472.
Morel B., Durand P., Jaffrezic A., Gruau G. and Molenat J. (2009) Sources of dissolved organic carbon during stormflow in a headwater agricultural catchment. *Hydrol. Process.* **23**, 2888–2901.
Mu C. C., Zhang T. J., Zhao Q., Guo H., Zhong W., Su H. and Wu Q. B. (2016) Soil organic carbon stabilization by iron in permafrost regions of the Qinghai-Tibet Plateau. *Geophys. Res. Lett.* **43**, 10286–10294.
Nelson M., Rhoades C. and Dwire K. (2011) Influence of bedrock geology on water chemistry of slope wetlands and headwater streams in the Southern Rocky Mountains. *Wetlands* **31**, 251–261.
Olivie-Lauquet G., Gruau G., Dia A., Riou C., Jaffrezic A. and Henin O. (2001) Release of trace elements in wetlands: role of seasonal variability. *Water Res.* **35**, 943–952.
Pallud C. and Van Cappellen P. (2006) Kinetics of microbial sulfate reduction in estuarine sediments. *Geochim. Cosmochim. Acta* **70**, 1148–1162.
Pallud C., Meile C., Laverman A. M., Abell J. and Van Cappellen P. (2007) The use of flow-through sediment reactors in biogeochemical kinetics: methodology and examples of applications. *Mar. Chem.* **106**, 256–271.
Pallud C., Masue-Slowey Y. and Fendorf S. (2010) Aggregate-scale spatial heterogeneity in reductive transformation of ferrihydrite resulting from coupled biogeochemical and physical processes. *Geochim. Cosmochim. Acta* **74**, 2811–2825.
Pan W., Kan J., Inamdar S., Chen C. and Sparks D. (2016) Dissimilatory microbial iron reduction release DCO (dissolved organic carbon) from carbon ferrihydrite association. *Soil Biol. Biochem.* **103**, 232–240.
Paul S., Küsel K. and Alewell C. (2006) Reduction processes in forest wetlands: tracking down heterogeneity of source/sink functions with a combination of methods. *Soil Biol. Biochem.* **38**, 1028–1039.
Peiffer S., Walton-Day K. and Macaladay D. L. (1999) The interaction of natural organic matter with iron in a wetland (Tennessee Park, Colorado) receiving acid mine drainage. *Aquat. Geochem.* **5**, 207–223.
Peng C., Sundman A., Bryce C., Catrouillet C., Borch T. and Kappler A. (2018) Oxidation of Fe(II)-organic-matter complexes in the presence of the mixotrophic nitrate-reducing Fe(II)-oxidizing bacterium *Acidovorax* sp. BoFeN1. *Environ. Sci. Technol.* **52**, 5753–5763.
Peng C., Bryce C., Sundman A., Borch T. and Kappler A. (2019) Organic matter complexation promotes Fe(II) oxidation by the photoautotrophic Fe(II)-oxidizer *Rhodopseudomonas palustris* TIE-1. *ACS Earth Space Chem.* **3**, 531–536.
Petruzzelli L., Celi L. and Ajmone-Marsan F. (2005) Effects of soil organic fraction on iron oxide biodissolution under anaerobic conditions. *Soil Sci.* **170**, 102–109.
R Core Team. (2016) R: A Language and Environment for Statistical Computing. R Foundation for Statistical Computing, Vienna, Austria.
Rhoades C. C., Battaglia M., Rocca M. and Ryan M. G. (2012) Short- and medium-term effects of fuel reduction mulch treatments on soil nitrogen availability in Colorado conifer forests. *Forest Ecol. Manag.* **276**, 231–238.
Rhoades C. C., Hubbard R. M. and Elder K. (2017) A decade of streamwater nitrogen and forest dynamics after a mountain pine beetle outbreak at the Fraser Experimental Forest Colorado. *Ecosys.* **20**, 380–392.
Richards C. and Pallud C. (2016) Kinetics of sulfate reduction and sulfide precipitation rates in sediments of a bar-built estuary (Pescadero, California). *Water Res.* **94**, 86–102.
Riedel T., Zak D., Biester H. and Dittmar T. (2013) Iron traps terrestrially derived dissolved organic matter at redox interfaces. *Proc. Natl. Acad. Sci. USA* **110**, 10101–10105.
Roden E. E. and Wetzel R. G. (1996) Organic carbon oxidation and suppression of methane production by microbial Fe(III) oxide reduction in vegetated and unvegetated freshwater wetland sediment. *Limnol. Oceanogr.* **41**, 1733–1748.
Roulet N. and Moore T. R. (2006) Environmental chemistry: browning the waters. *Nature* **444**, 283–284.
Scharlemann J. P., Tanner E. V., Hiederer R. and Kapos V. (2014) Global soil carbon: understanding and managing the largest terrestrial carbon pool. *Carbon Manag.* **5**, 81–91.
Schiff S. L., Aravena R., Trumbore S. E., Hinton M. J., Elgood R. and Dillon P. J. (1997) Export of DOC from forested catchments on the Precambrian Shield of central Ontario: clues form ^{13}C and ^{14}C. *Biogeochemistry* **36**, 43–65.
Schilling K., Borch T., Rhoades C. C. and Pallud C. E. (2019) Temperature sensitivity of microbial Fe(III) reduction kinetics in subalpine wetland soils. *Biogeochem.* **142**, 19–35.
Segnini A., Posadas A., Quiroz R., Milori D. M. B. P., Saab S. C., Neto L. M. and Vaz C. M. P. (2010) Spectroscopic assessment of soil organic matter in wetlands from the high Andes. *Soil Sci. Soc. Am. J.* **74**, 2246–2253.
Shimizu M., Zhou J., Schröder C., Obst M., Kappler A. and Borch T. (2013) Dissimilatory reduction and transformation of ferrihydrite-humic acid coprecipitates. *Environ. Sci. Technol.* **47**, 13375–13384.
Stookey L. (1970) Ferrozine–A new spectrophotometric reagent for iron. *Anal Chem.* **42**, 779–781.
Striegl R. G., Aiken G. R., Dornblaser M. M., Raymond P. A. and Wickland K. P. (2005) A decrease in discharge-normalized DOC export by the Yukon River during summer through autumn. *Geophys. Res. Lett.* **32**, 1–4.
Striegl R. G., Dornblaser M. M., McDonald C. P., Rover J. R. and Stets E. G. (2012) Carbon dioxide and methane emissions from the Yukon River system. *Global Biogeochem Cycles.* **26**, GB0E05. https://doi.org/10.1029/2012GB004306.
Sumner M. E. and Miller W. P. (2005) Cation exchange capacity and exchange coefficients. In *Methods of Soil Analysis, Part 3 Chemical Methods* (ed. D. L. Sparks). Soil Science Society of America, Madison, pp. 1201–1230.

Thomas G. W. (2005) Soil pH and soil acidity. In *Methods of Soil Analysis, Part 3 Chemical Methods* (ed. D. L. Sparks). Soil Science Society of America, Madison, pp. 475–490.

Tranvik L. J. and Jansson M. (2002) Terrestrial export of organic carbon. *Nature* **415**, 861–862.

Urban N. R., Brezonik P. L., Baker L. and Sherman L. (1994) Sulfate reduction and diffusion in sediments of Little Rock Lake, Wisconsin. *Limnol. Oceanogr.* **39**, 797–815.

Wagai R. and Mayer L. M. (2007) Sorptive stabilization of organic matter in soils by hydrous iron oxides. *Geochim. Cosmochim. Acta* **71**, 25–35.

Wallenstein M. D. and Hall E. K. (2012) A trait-based framework for predicting when and where microbial adaptation to climate change will affect ecosystem functioning. *Biogeochemistry* **109**, 35–47.

Winterdahl M., Futter M., Köhler S., Laudon H., Seibert J. and Bishop K. (2011) Riparian soil temperature modification of the relationship between flow and dissolved organic carbon concentration in a boreal stream. *Water Resour. Res.* **47**, 1–17.

Worrall F. and Burt T. (2004) Time series analysis of long-term river dissolved organic carbon records. *Hydrol. Process* **18**, 893–911.

Worrall F., Harriman R., Evans C. D., Watts C. D., Adamson J., Neal C., Tipping E., Burt T., Grieve I., Monteith D., Naden P. S., Nisbet T., Reynolds B. and Stevens P. (2004) Trends in dissolved organic carbon in UK rivers and lakes. *Biogeochemistry* **70**, 369–402.

Zarnetske J. P., Bouda M., Abbott B. W., Saiers J. and Raymond P. A. (2018) Generality of hydrologic transport limitation of watershed organic carbon flux across ecoregions of the United States. *Geophys. Res. Lett.* **45**, 11702–11711.

Zhou Z., Latta D., Noor N., Thompson A., Borch T. and Scherer M. (2018) Fe(II)-catalyzed transformation of organic matter-ferrihydrite coprecipitates: a closer look using Fe isotopes. *Environ. Sci. Technol.* **52**, 11142–11150.

Associate editor: Oleg Pokrovsky